

## Design tables and charts for uniform and non-uniform tuned liquid column dampers in harmonic pitching motion

Jong-Cheng Wu\*<sup>1</sup>, Yen-Po Wang<sup>2</sup> and Yi-Hsuan Chen<sup>2</sup>

<sup>1</sup>Department of Civil Engineering, Tamkang University, Taipei, Taiwan

<sup>2</sup>Department of Civil Engineering, National Chiao Tung University, Hsinchu, Taiwan

(Received January 31, 2011, Revised January 29, 2012, Accepted February 2, 2012)

**Abstract.** In the first part of the paper, the optimal design parameters for tuned liquid column dampers (TLCD) in harmonic pitching motion were investigated. The configurations in design tables include uniform and non-uniform TLCDs with cross-sectional ratios of 0.3, 0.6, 1, 2 and 3 for the design in different situations. A closed-form solution of the structural response was used for performing numerical optimization. The results from optimization indicate that the optimal structural response always occurs when the two resonant peaks along the frequency axis are equal. The optimal frequency tuning ratio, optimal head loss coefficient, the corresponding response and other useful quantities are constructed in design tables as a guideline for practitioners. As the value of the head loss coefficient is only available through experiments, in the second part of the paper, the prediction of head loss coefficients in the form of a design chart are proposed based on a series of large scale tests in pitching base motions, aiming to ease the predicament of lacking the information of head loss for those who wishes to make designs without going through experimentation. A large extent of TLCDs with cross-sectional ratios of 0.3, 0.6, 1, 2 and 3 and orifice blocking ratios ranging from 0%, 20%, 40%, 60% to 80% were inspected by means of a closed-form solution under harmonic base motion for identification. For the convenience of practical use, the corresponding empirical formulas for predicting head loss coefficients of TLCDs in relation to the cross-sectional ratio and the orifice blocking ratio were also proposed. For supplemental information to horizontal base motion, the relation of head loss values versus blocking ratios and the corresponding empirical formulas were also presented in the end.

**Keywords:** tuned liquid column damper; frequency tuning ratio; head loss coefficient; cross-sectional ratio; pitching motion.

---

### 1. Introduction

Since Sakai and his co-authors developed the idea of tuned liquid column damper (TLCD) for the purpose of vibration suppression (Sakai *et al.* 1989), many successors have used it in civil engineering applications and verified its control effectiveness in the past decades. Although most relevant literature focused on building applications where the TLCDs sway horizontally (e.g., Xu *et al.* 1992, Won *et al.* 1997, Gao *et al.* 1997, Hitchcock *et al.* 1997, Balendra *et al.* 1995, Balendra *et al.* 1999a, Balendra *et al.* 1999b, Chang *et al.* 1998, Chang 1999, Yalla *et al.* 2000, Wu *et al.* 2005, Wu *et al.* 2009, Heo *et al.* 2009, Chang 2011, Chakraborty and Debbarma 2011, Debbarma *et al.* 2011, Li *et al.* 2011), some attention has been recently extended to the application to bridge deck control (e.g.,

---

\*Corresponding author, Professor, E-mail: [joncheng@mail.tku.edu.tw](mailto:joncheng@mail.tku.edu.tw)

Xue *et al.* 2000a, Xue *et al.* 2000b, Taflanidis *et al.* 2005, Wu *et al.* 2008, Shum *et al.* 2002, Xu *et al.* 2003). The bridge deck control concerns the response of bridge deck in the pitching (torsional) direction which involves TLCs in rotational motion. In fact, no matter the motion is horizontal or rotational, such a device indeed has the advantages over other types of energy-dissipating dampers due to its mechanism simplicity. For instance, its natural frequency is simply determined by the length of the liquid column, and the generating mechanism of its damping is due to the head loss of the flow motion in the U shape of columns.

In applying this device toward actual implementation, the determination of the optimal parameters, such as the optimal frequency tuning ratio and optimal head loss coefficient, is an imminent issue that should be investigated. Some papers had contributed useful information on them for horizontal motion (Balendra *et al.* 1995, Chang *et al.* 1998, Chang 1999, Yalla *et al.* 2000, Wu *et al.* 2005, Wu *et al.* 2009). Particularly interesting fact was shown in Wu *et al.* (2005) and Wu *et al.* (2009) that, under the same horizontal length ratio, a uniform TLC is always better than a non-uniform TLC in the optimal condition (TLC with non-uniform liquid columns was first termed as Liquid Column vibration Absorber (LCVA) in Hitchcock *et al.* (1997)). However, the designs of non-uniform TLCs are still in practice on some occasions for particular reasons. For instance, in the space-restricted area, a way to shorten the horizontal space requirement is to choose the cross-sectional ratio (vertical versus horizontal) larger than 1. In the situation where a higher frequency is to be tuned, the resulting short horizontal liquid column length might be too close to the dimension of TLC cross sections. In that case, the solution is to choose the cross-sectional ratio smaller than 1. Therefore for the general purpose, the investigation of non-uniform TLCs is worthwhile.

For bridge structures equipped with uniform TLCs subject to pitching moment, the equations of motion was first presented by Xue *et al.* (2000a). The determination of optimal parameters, including frequency tuning ratio and head loss coefficient, was investigated by Xue *et al.* (2000b) by considering undamped structures equipped with uniform TLCs responding to harmonic loading. For situations under white noise loading, the optimal parameters were presented by Taflanidis *et al.* (2005) based on the equation of motion presented in Xue *et al.* (2000a). Later, when the interaction mechanism was revisited for extending to non-uniform TLCs by strictly following the energy principle, it was intriguingly found by Wu *et al.* (2008) that the equation of motion in the structural part should contain an additional term, which is somehow not revealed in Xue *et al.* (2000a), Xue *et al.* (2000b) and Taflanidis *et al.* (2005). Therefore in the first part of this paper, the optimal parameters of TLCs equipped in damped structures using the corrected equations of motion in Wu *et al.* (2008) under harmonic pitching moment are re-investigated and arranged in design tables for the purpose of practical use. The numerical optimization is performed by directly minimizing the peak structural (pitching) amplitude over all possible frequencies using a closed-form solution. For the general purpose, the design tables include uniform and non-uniform TLCs with cross-sectional ratios of 0.3, 0.6, 1, 2 and 3.

It is noted that the value of the head loss coefficient is only available through experiments. To ease the predicament of lacking such information for practitioners, the second part of this paper aims to provide their design charts identified from a series of large scale tests for TLCs with cross-sectional ratios of 0.3, 0.6, 1, 2 and 3. For the convenience of practical use, the corresponding empirical formulas for predicting head loss coefficients of TLCs in relation to the cross-sectional ratio and the orifice blocking ratio are also proposed.

## 2. Formulation

### 2.1 Equation of motion with a TLCD in the pitching direction

The schematic diagram of a single-degree-of-freedom structure equipped with a TLCD subjected to pitching motion is shown in Figs. 1(a) and (b), depending on whether the horizontal column of the TLCD is located below ( $e$  is positive) or above ( $e$  is negative) the rotational center of the structure. The establishment of the liquid response in TLCDs is based on the following assumptions (i) the sloshing behavior on the liquid surface is negligible; (ii) the flow is incompressible (i.e., flow rate is constant), depicting that water is a good choice; (iii) the in-plane width of the column cross-section in the TLCD should be much smaller than its horizontal length.

According to Wu *et al.* (2008), the equation of motion of a SDOF structure equipped with a TLCD subjected to pitching motion can be expressed as

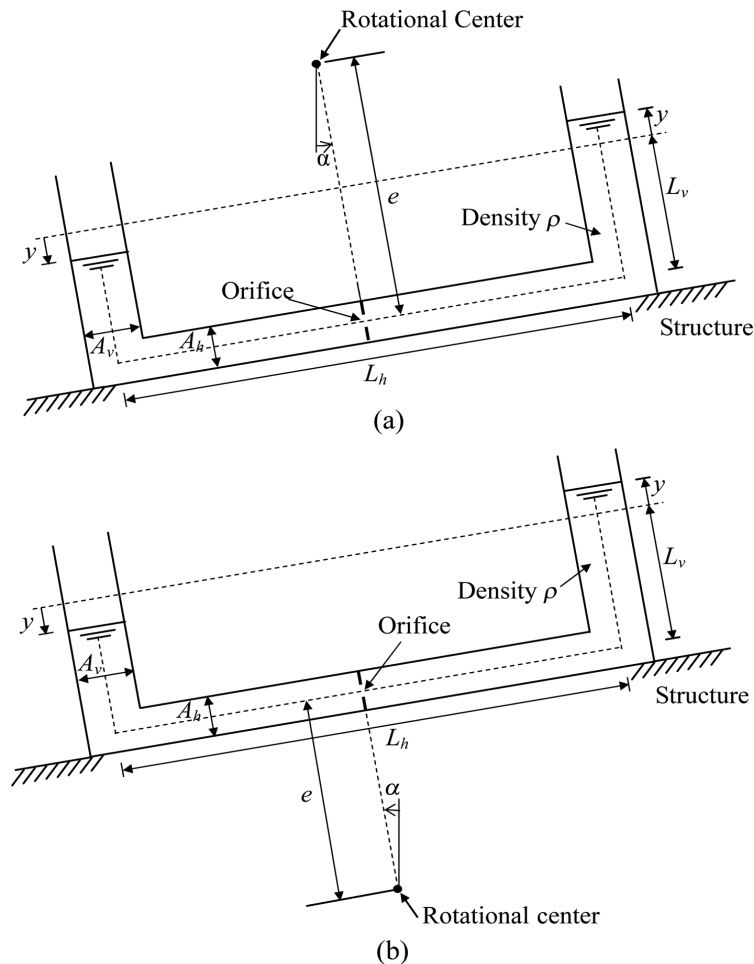


Fig. 1 A TLCD in rotational motion: (a) horizontal column of a TLCD is located below the rotational center ( $e$  is positive) and (b) horizontal column of a TLCD is located above the rotational center ( $e$  is negative)

$$(J_d + J_\alpha)\ddot{\alpha} + C_\alpha\dot{\alpha} + K_\alpha\alpha + \rho v A_h L_h (L_v + e)\ddot{y} + \rho g A_h (L_h + 2vL_v)e\alpha + \rho g v A_h L_h y - \rho g v A_h L_v^2 \alpha = M(t) \quad (1)$$

and

$$\rho v A_h L_h (L_v + e)\ddot{\alpha} + \rho v A_h (2L_v + vL_h)\ddot{y} + \frac{1}{2}\rho\eta v^2 A_h \dot{y}|\dot{y}| + \rho g v A_h L_h \alpha + 2\rho g v A_h y = 0 \quad (2)$$

in which  $\alpha$  and  $y$  denote the pitching angle of the structure and liquid displacement in the TLCD, respectively;  $J_\alpha$  is the mass moment of inertia of the structure with respect to the rotational center;  $J_d = \rho A_h [(1/2)vL_v L_h^2 + 2v e^2 L_v - 2v e L_v^2 + (2/3)vL_v^3 + L_h e^2 + (1/12)L_h^3]$  is the mass moment of inertia of the fluid contained in a TLCD with respect to the rotational center;  $K_\alpha$  is the rotational stiffness constant of the structure;  $g$  is acceleration due to gravity;  $\rho$  is the fluid density;  $A_h$  ( $A_v$ ) and  $L_h$  ( $L_v$ ) are the cross-sectional area and column length of the horizontal (vertical) liquid columns;  $e$  is the vertical distance between the rotational center of the structure and the horizontal liquid column;  $\nu = A_v/A_h$  is the cross-section ratio of the vertical column versus horizontal column;  $\eta$  is the so-called head loss coefficient; and  $M(t)$  is the external moment. Noted that the last term  $-\rho g v A_h L_v^2 \alpha$  in Eq. (1) is the additional term that was not revealed in the existent literature Xue *et al.* (2000a), Xue *et al.* (2000b) and Taflanidis *et al.* (2005). Since this additional term is a linear function of  $\alpha$ , it will contribute an extra stiffness to the structure and therefore alter the natural frequency of the structure.

In the case that the structural motion  $\alpha$  is specified, the liquid motion in the TLCD can be determined by Eq. (2) only. As such, the natural frequency of a TLCD can be easily shown as  $\omega_d = \sqrt{2g/L_e}$ , in which  $L_e = 2L_v + vL_h$  is defined as the effective length of liquid column. Consequently, the natural period of a TLCD,  $T_d$ , is  $T_d = 2\pi\sqrt{L_e/2g}$ . Note that the effective length  $L_e$  is equal to the total length  $L$  of the liquid column if the cross-section is uniform (i.e.,  $\nu=1$ ).

Since this paper conducted a basic research on the interaction between a structure and TLCD in pitching motion, a single-degree-of-freedom structure is used for simplicity. For a multiple-degree-of-freedom system with a certain dominant torsional mode, the torsional modal equation should be obtained by performing the modal decomposition technique with the torsional mode shape component at the location where the TLCD is installed set to one. Then the corresponding modal mass, stiffness and damping will be used as the structural properties in the formula described above.

## 2.2. Nondimensionalization for equations of motion

To perform parametric analysis, nondimensionalization for the equations of motion in Eqs. (1) and (2) should be performed beforehand and the resultant equations (Wu *et al.* 2008) are expressed by

$$(1 + \mu)\alpha'' + 4\pi\xi\beta_1\alpha' + 4\pi^2\beta_1^2\alpha + \frac{v\varepsilon r}{p}\hat{y}'' + 2\pi^2\frac{v\varepsilon q}{mn}\alpha + 2\pi^2\frac{v\varepsilon}{n}\hat{y}' - \frac{\pi^2 v\varepsilon}{2n}\left(\frac{1}{p} - 1\right)^2\alpha = \hat{M}(\hat{t}) \quad (3)$$

$$\frac{nr}{p}\alpha'' + \hat{y}'' + \frac{1}{2}v n \eta|\hat{y}'|\hat{y}' + 2\pi^2\alpha + 4\pi^2\hat{y} = 0 \quad (4)$$

in which  $(\hat{\cdot})$  represents the differentiation with respect to  $\hat{t}=t/T_d$ . Other nondimensional quantities are defined as follows:  $\hat{y} = y/L_h$ ;  $\hat{M}(\hat{t})=M T_d^2/J_\alpha$ ;  $\beta_1 = \omega_\alpha/\omega_d$  is the natural frequency ratio of the structure versus TLCD ( $\omega_\alpha = \sqrt{K_\alpha/J_\alpha}$  is the structural natural frequency);  $\xi = C_\alpha/2J_\alpha \omega_\alpha$  is the structural damping ratio;  $p = L_h/L$  is the ratio of the horizontal column length versus total length of a TLCD;  $q = e/L_h$  is the rotational center position ratio which is the ratio of the distance between the

rotational center and horizontal column versus the TLCD horizontal column length;  $m$  and  $n$  are two parameters related to  $p$  and  $\nu$  (i.e.,  $m = \nu p / (\nu + p(1 - \nu))$  is the ratio of  $\nu L_h$  versus  $(L_h + 2\nu L_v)$  and  $n = p / (1 - p(1 - \nu))$  is the ratio of  $L_h$  versus  $L_e$ );  $r = pq + (1 - p)/2$  is a parameter depending on  $p$  and  $q$ ;  $\mu = J_d / J_\alpha$  is the ratio of mass moment of inertia of the TLCD versus structure; and  $\varepsilon = \rho A_h L_h^3 / J_\alpha$ . The parameters  $\mu$  and  $\varepsilon$  are related to each other by  $\mu = \varepsilon \left[ \frac{1}{2} \nu \left( \frac{1-p}{2p} \right) + 2\nu q^2 \left( \frac{1-p}{2p} \right) - 2\nu q \left( \frac{1-p}{2p} \right)^2 + \frac{2}{3} \nu \left( \frac{1-p}{2p} \right)^3 + q^2 + \frac{1}{12} \right]$ , which can be obtained by expressing  $J_d$  as a function of  $\varepsilon$ ,  $p$ ,  $q$  and  $\nu$  (Wu *et al.* 2008). It is noticed that the term  $-\frac{\pi^2 \nu \varepsilon}{2n} \left( \frac{1}{p} - 1 \right)^2 \alpha$  in Eq. (3) is corresponding to  $-\rho g \nu A_h L_v^2 \alpha$  in Eq. (1), which is the additional term revealed in Wu *et al.* (2008) in the dimensionless form.

### 2.3 Equivalent viscous damping under harmonic loading

If a system is subjected to a harmonic type of loading, the nonlinear damping force term  $(1/2)\rho\eta\nu^2 A_h \dot{y} |\dot{y}|$  in Eq. (2) can be replaced by an equivalent viscous damping force expressed as  $\frac{4}{3\pi} \rho\eta\nu^2 A_h \varphi_y \omega \dot{y}$ , in which  $\varphi_y$  is the amplitude of liquid displacement  $y$  and  $\omega$  is the circular excitation frequency (see Gao *et al.* 1997). Thus, the nondimensionalized equation in Eq. (4) can be rewritten as

$$\frac{nr}{p} \alpha'' + \hat{y}'' + \frac{8}{3} \nu n \eta \varphi_y k \hat{y}' + 2\pi^2 \alpha + 4\pi^2 \hat{y} = 0 \quad (5)$$

in which  $k = \omega/\omega_d$  is the ratio of the excitation frequency versus TLCD natural frequency (excitation frequency ratio); and  $\varphi_y = \varphi_y/L_h$  is the nondimensionalized amplitude of the liquid displacement.

### 2.4 Closed-form solution to harmonic pitching moment

According to Wu *et al.* (2008), the closed-form solution of Eqs. (3) and (5) can be obtained by

$$|\alpha_0|^2 = \frac{T_F \cdot \hat{M}_0^2}{(T_B + T_C \cdot |\hat{y}_0|)^2 + (T_D + T_E \cdot |\hat{y}_0|)^2} \quad (6)$$

in which

$$T_B = 8\pi^2(1 - k^2) \left[ \beta_1^2 - k^2(1 + \mu) + \frac{\nu \varepsilon q}{2mn} - \frac{\nu \varepsilon}{8n} \left( \frac{1}{p} - 1 \right)^2 \right] - 2\pi^2 \varepsilon \left( \frac{\nu}{n} - 4k^2 \frac{\nu r}{p} + 4k^4 \frac{\nu n r^2}{p^2} \right) \quad (7)$$

$$T_C = -\frac{64}{3} \pi k^3 \nu n \eta \zeta \beta_1; \quad T_D = 16\pi^2 k \zeta \beta_1 (1 - k^2) \quad (8)$$

$$T_E = \frac{32}{3} \pi k^2 \nu n \eta \left[ \left( \beta_1^2 + \frac{\nu \varepsilon q}{2mn} \right) - k^2(1 + \mu) - \frac{\nu \varepsilon}{8n} \left( \frac{1}{p} - 1 \right)^2 \right] \quad (9)$$

$$T_F = 4(1 - k^2)^2 + \left( \frac{8}{3\pi} k^2 \nu n \eta |\hat{y}_0| \right)^2 \quad (10)$$

In Eq. (6),  $|\hat{y}_0|$  is obtained by solving a polynomial expressed as

$$C_4 |\hat{y}_0|^4 + C_3 |\hat{y}_0|^3 + C_2 |\hat{y}_0|^2 + C_0 = 0 \quad (11)$$

in which

$$C_4 = T_C^2 + T_E^2; C_3 = 2(T_B \cdot T_C + T_D \cdot T_E)$$

$$C_2 = T_B^2 + T_D^2; C_0 = -T_A \cdot \hat{M}_0^2 \quad (12)$$

$$T_A = \left(2k^2 \frac{nr}{p} - 1\right)^2 \quad (13)$$

It can be shown by extensive simulation from Eq. (11) that  $|\hat{y}_0|$  has a unique positive or zero solution.

### 3. Optimization

#### 3.1 Performance index

In most civil engineering applications, the excitation frequency from harmonic disturbance (such as vortex shedding in the across-wind direction) usually varies and is not certain. Hence it is more reasonable to consider the worst case of structural response in all possible frequencies while response is minimized. Let the normalized structural and liquid responses be defined as

$$[\alpha_0]_{norm} = |\alpha_0|/\alpha_{p(original)} \quad (14)$$

and

$$[\hat{y}_0]_{norm} = |\hat{y}_0|/\alpha_{p(original)} \quad (15)$$

in which  $\alpha_{p(original)}$  is the original structural peak amplitude (worst case) over all possible frequencies. In fact, the value of  $\alpha_{p(original)}$  can be derived from the equation of motion of the original structure, i.e., Eq. (3) with keeping only first three terms and  $\mu = 0$

$$\alpha_{p(original)} = \frac{\hat{M}_0}{4\pi^2\beta_1^2} \cdot \frac{1}{2\xi\sqrt{1-\xi^2}} \quad (16)$$

With this, the performance index (*P.I.*) is defined as the peak amplitude (worst case) of  $[\alpha_0]_{norm}$  over all possible frequencies, i.e.,

$$P.I. = [\alpha_p]_{norm} = \text{Max}_{k \in R} [\alpha_0]_{norm} \quad (17)$$

According to this definition, the optimization (minimization) on the performance index can be categorized as a kind of the so-called Min-Max problem in which  $[\alpha_p]_{norm}$  is actually the  $H_\infty$  norm of  $[\alpha_0]_{norm}$  in Eq. (14) (Skelton 1988). A smaller  $[\alpha_p]_{norm}$  represents a better performance.

In addition, the overall effective damping ratio  $\xi_e$  for the structure can be calculated by equating  $[\alpha_p]_{norm} \cdot \alpha_{p(original)}$  to  $\frac{\hat{M}_0}{4\pi^2\beta_1^2} \cdot \frac{1}{2\xi_e\sqrt{1-\xi_e^2}}$ . The substitution of Eq. (16) leads to

$$\xi_e^4 - \xi_e^2 + \xi_e^2(1 - \xi_e^2)/[\alpha_p]_{norm}^2 = 0 \quad (18)$$

Hence, the equivalent damping ratio  $\xi_e$  can be obtained by

$$\xi_e = \left( \frac{1 - \sqrt{1 - 4\xi^2(1 - \xi^2) / [\alpha_p]_{norm}^2}}{2} \right)^{1/2} \approx \frac{\xi}{[\alpha_p]_{norm}} \quad (19)$$

A larger  $\xi_e$  represents better performance.

Similarly, the normalized peak amplitude (worst case) of  $[\hat{y}_0]_{norm}$  over all possible frequencies can be also defined as

$$[\hat{y}_p]_{norm} = \text{Max}_{k \in R} [\hat{y}_0]_{norm} \quad (20)$$

The value of  $[\hat{y}_p]_{norm}$  is to be used for checking if the liquid surface displacement exceeds the length of the vertical liquid column.

### 3.2 Determination of optimal parameters $\beta_1$ and $\eta$

As shown in Eqs. (14) and (17), the independent parameters for determining  $[\alpha_p]_{norm}$  include the structural damping ratio  $\xi$ , mass ratio  $\mu$ , cross-section ratio  $\nu$ , horizontal length ratio  $p$ , rotational center position ratio  $q$ , non-dimensional external moment amplitude  $\hat{M}_0$ , head loss coefficient  $\eta$  and frequency tuning ratio  $\beta_1$ . Since the structural damping ratio  $\xi$  and  $\hat{M}_0$  shall be known as a *priori* in the application, and the mass ratio  $\mu$ , cross-section ratio  $\nu$ , horizontal length ratio  $p$ , and rotational center position ratio  $q$  depend on the choices of the designer, the parameters remained to be optimized are actually  $\beta_1$  and  $\eta$ .

A numerical optimization techniques such as the gradient method can be used to locate the optimal parameters  $\eta$  and  $\beta_1$ . In this paper, the program “fminsearch” in the software MATLAB was used. From the results of extensive numerical optimization, it was indicated that the minimal  $[\alpha_p]_{norm}$  (i.e., the optimal case) always occurs when the two resonant peaks along the frequency axis are equal, and this applies to both damped and undamped structures. To demonstrate this observation, the plots of  $[\alpha_0]_{norm}$  and  $[\hat{y}_0]_{norm}$  versus the non-dimensional excitation frequency  $k$  are shown in Fig. 2 for a damped structure ( $\nu=2$ ,  $\xi=2\%$ ,  $\mu=0.5\%$ ,  $p=0.7$ ,  $q=-0.3$  and  $\hat{M}_0=0.01$ ) and the plots of  $|\alpha_0|$  and  $|\hat{y}_0|$  versus the non-dimensional excitation frequency  $k$  are shown in Fig. 3 for an undamped structure ( $\nu=2$ ,  $\xi=0$ ,  $\mu=0.5\%$ ,  $p=0.7$ ,  $q=-0.3$  and  $\hat{M}_0=0.01$ ). The plots for the optimal cases ( $\beta_{1opt}=1.0085$ ,  $\eta_{opt}=62.536$  in Fig. 2 and  $\beta_{1opt}=1.0066$ ,  $\eta_{opt}=39.6159$  in Fig. 3) were denoted by the black solid curves, while the other two curves represent the cases using other values of  $\eta$  but keeping  $\beta_1$  optimal. In the optimal case, the frequencies at  $k_1$ ,  $k_2$  and  $k_3$  as denoted in Figs. 2(a) and (b) are three important frequencies that provide useful information on the excitation frequencies where the worst cases occur. They will be given in the lists of design tables presented in Section 3.3.

The extensive numerical results further reveal two important findings, which are described in the following.

(1) For an undamped structure, by varying the value of  $\eta$  but keeping  $\beta_1$  the same, there exist two invariant points in  $|\alpha_0|$  plot and one invariant point in  $|\hat{y}_0|$  plot. As shown in Fig. 3, the two invariant points in the  $|\alpha_0|$  plot even share the same amplitude when the optimal  $\beta_1$  is adopted, which is actually the criterion used in the Den Hartog approach for determining the optimal tuning ratio for TMDs (Den Hartog 1956).

(2) The optimal head loss is inversely proportional to external moment amplitude which however

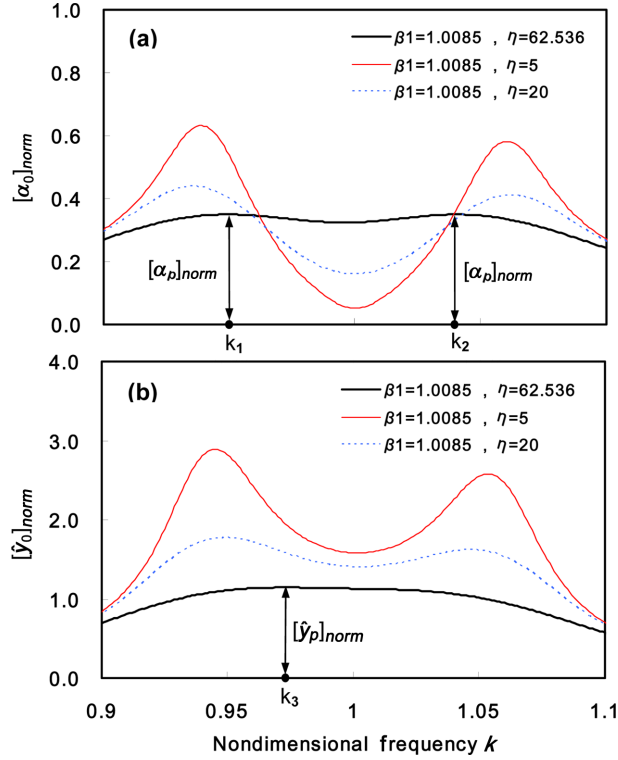


Fig. 2 Demonstrative plots of  $[\alpha_0]_{norm}$  and  $[\hat{y}_0]_{norm}$  for a damped structure (with Parameters  $\nu=2$ ,  $\xi=2\%$ ,  $\mu=0.5\%$ ,  $p=0.7$ ,  $q=-0.3$ ,  $\hat{M}_0=0.01$ ): (a)  $[\alpha_0]_{norm}$  versus  $k$  and (b)  $[\hat{y}_0]_{norm}$  versus  $k$

has no effect on the optimal tuning ratio  $\beta_1$ ,  $[\alpha_p]_{norm}$  and  $[\hat{y}_p]_{norm}$ . In fact, this can be observed theoretically. Because of the co-occurrence of  $\eta|\hat{y}_0|$  in Eqs. (6)-(10), the values of  $|\hat{y}_0|$  and  $|\alpha_0|$  solved from Eqs. (11) and Eq. (6) are proportional to  $\hat{M}_0$  as long as  $\eta|\hat{y}_0|$  remains constant. Thus, the external force amplitude  $\hat{M}_0$  has no effect on the optimal tuning ratio  $\beta_{1opt}$  and the associated values of  $[\alpha_p]_{norm}$ ,  $[\hat{y}_p]_{norm}$ ,  $\xi_e$ ,  $k_1$ ,  $k_2$  and  $k_3$ . But a constant value of  $\eta|\hat{y}_0|$  implies that the optimal head loss coefficient  $\eta_{opt}$  is inversely proportional to  $|\hat{y}_0|$  and thus the moment amplitude  $\hat{M}_0$ .

### 3.3 Design tables

In this section, design tables containing the lists of the optimal parameters for uniform ( $\nu=1$ ) and non-uniform TLCDs ( $\nu=2, 3, 0.6, 0.3$ ) were presented in Tables 1 and 2~5, respectively, as quick guidelines for practical use. In these tables, the practical ranges considered for the horizontal length ratio  $p$  and the structural damping ratio  $\xi$  are 0.6-0.8 and 1%-2%, respectively. Aside from the optimal parameters  $\beta_{1opt}$  and  $\eta_{opt}$ , the associated values of  $[\hat{x}_p]_{norm}$ ,  $[\hat{y}_p]_{norm}$ ,  $\xi_e$  and  $k_1$ ,  $k_2$  and  $k_3$  as defined in Fig. 2 were all tabulated as the necessary information for design. Since a larger ratio of mass moment of inertia  $\mu$  will increase the control performance, in considering a reasonable performance, for the cases of  $\nu \geq 1$  (Tables 1-3), the range for the ratio of mass moment of inertia  $\mu$  is 0.25%-0.5%, whereas the rotational center position ratio  $q$  has three variations of -0.3, 0 and 0.3 as the design choices. As compared between Tables 1-3, when the cross-section ratio  $\nu$  becomes

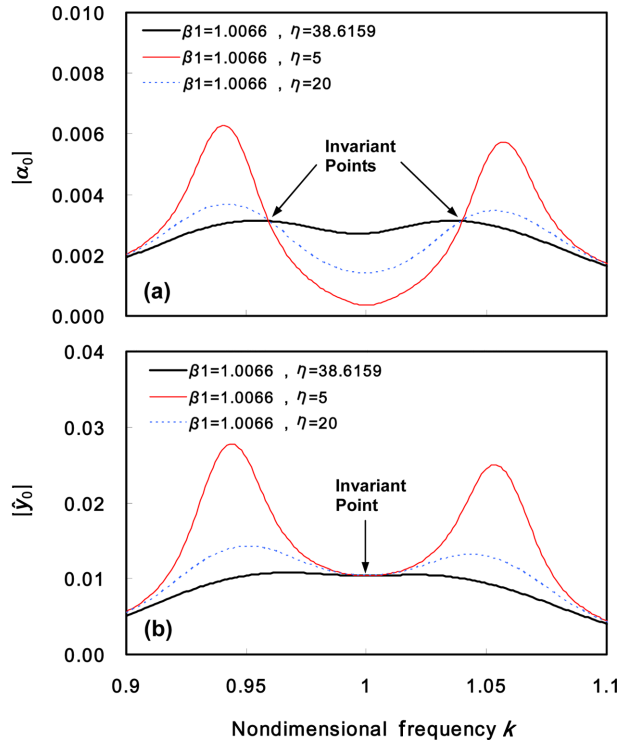


Fig. 3 Demonstrative plots of  $|\alpha_0|$  and  $|\hat{y}_0|$  for an undamped structure (with Parameters  $\nu=2$ ,  $\xi=0$ ,  $\mu=0.5\%$ ,  $p=0.7$ ,  $q=-0.3$ ,  $M_0=0.01$ ): (a)  $|\alpha_0|$  versus  $k$  and (b)  $|\hat{y}_0|$  versus  $k$

bigger, a better performance can be achieved. Notice that choosing  $\nu$  larger than 1 is normally used in the situation when the horizontal space requirement for TLCDs is restricted.

For the other two cases of  $\nu=0.6$  (Table 4) and  $\nu=0.3$  (Table 5), to retain a reasonable performance, the range for the ratio of mass moment of inertia  $\mu$  is increased to 0.5%-1% and 1%-2%, respectively, whereas the choices for the rotational center position ratio  $q$  has changed to -0.3, -0.15 and 0. In these cases, the use of a positive  $q$  does not show significant control effectiveness. Choosing  $\nu$  smaller than 1 is rarely suggested because of worse performance. However, in the situation when a higher frequency is to be tuned, the resulting short horizontal liquid column length might be too close to the dimension of TLCD cross-sections. In that case, the solution is to choose  $\nu$  smaller than 1.

#### 4. Identification of head loss coefficients

There exist a few causes of TLCD head loss generation because of its shape, including those induced by (1) the flow through the turn elbow, (2) the enlargement or contraction of the cross-sectional variation during flow motion, (3) the resistance from flow passing an orifice that resides in the middle of the horizontal column (see Fig. 4), and (4) the viscosity between the fluid and column wall. In practice, it is difficult to identify the individual head loss induced by each cause. In fact, the head loss due to the cause (1) can be lumped into that of the cause (2), i.e., the effect of cross-sectional ratios, since TLCDs considered herein are all configured with turn elbows in 90 degrees.

Table 1 Optimal parameters for uniform TLCD designs in pitching motion with  $\nu=1$ 

$\nu=1, \xi=1\%, \mu=0.25\%$							
$p$ (1)	$q$ (2)	$\frac{1}{\beta_{1opt}} = \frac{\omega_d}{\omega_s}$ (3)	$\eta_{opt} (\times 10^{-2}/\hat{M}_0)$	$[\alpha_p]_{norm}$	$[\hat{y}_p]_{norm}$	$\xi_e(\%)$	$k_{1,2,3}=\omega_{1,2,3}/\omega_d$
0.6	-0.3	0.9971	6.076	0.410	3.073	2.44	0.981, 1.018, 0.993
	<b>0.0</b>	<b>0.9986</b>	<b>6.355</b>	<b>0.456</b>	<b>2.520</b>	<b>2.19</b>	<b>0.983, 1.014, 0.995</b>
	0.3	1.0002	1.428	0.727	4.279	1.38	0.993, 1.006, 0.999
0.7	<b>-0.3</b>	<b>0.9969</b>	<b>8.404</b>	<b>0.350</b>	<b>2.416</b>	<b>2.86</b>	<b>0.976, 1.021, 0.990</b>
	0.0	0.9988	8.486	0.393	2.015	2.55	0.979, 1.017, 0.991
	<b>0.3</b>	<b>1.0003</b>	<b>1.550</b>	<b>0.687</b>	<b>4.000</b>	<b>1.46</b>	<b>0.992, 1.007, 0.999</b>
0.8	-0.3	0.9965	10.972	0.303	1.968	3.30	0.972, 1.026, 0.986
	<b>0.0</b>	<b>0.9987</b>	<b>11.204</b>	<b>0.340</b>	<b>1.631</b>	<b>2.94</b>	<b>0.975, 1.021, 0.988</b>
	0.3	1.0003	1.669	0.649	3.741	1.54	0.991, 1.008, 0.999
$\nu=1, \xi=1\%, \mu=0.5\%$							
0.6	-0.3	0.9946	14.981	0.326	1.752	3.07	0.974, 1.023, 0.987
	<b>0.0</b>	<b>0.9975</b>	<b>15.250</b>	<b>0.367</b>	<b>1.461</b>	<b>2.72</b>	<b>0.976, 1.018, 0.989</b>
	0.3	1.0005	3.119	0.642	2.724	1.56	0.990, 1.007, 0.998
0.7	<b>-0.3</b>	<b>0.9941</b>	<b>20.924</b>	<b>0.273</b>	<b>1.357</b>	<b>3.66</b>	<b>0.967, 1.028, 0.982</b>
	0.0	0.9978	21.003	0.310	1.142	3.23	0.970, 1.022, 0.984
	<b>0.3</b>	<b>1.0006</b>	<b>3.351</b>	<b>0.597</b>	<b>2.531</b>	<b>1.67</b>	<b>0.989, 1.009, 0.997</b>
0.8	-0.3	0.9934	27.790	0.234	1.090	4.28	0.960, 1.034, 0.977
	<b>0.0</b>	<b>0.9977</b>	<b>28.219</b>	<b>0.265</b>	<b>0.910</b>	<b>3.78</b>	<b>0.964, 1.027, 0.979</b>
	0.3	1.0006	3.675	0.556	2.331	1.80	0.987, 1.010, 0.997
$\nu=1, \xi=2\%, \mu=0.25\%$							
0.6	-0.3	0.9965	9.351	0.597	4.279	3.35	0.979, 1.019, 0.996
	<b>0.0</b>	<b>0.9983</b>	<b>10.353</b>	<b>0.643</b>	<b>3.354</b>	<b>3.11</b>	<b>0.981, 1.016, 0.996</b>
	0.3	1.0001	3.195	0.857	4.445	2.33	0.991, 1.007, 0.999
0.7	<b>-0.3</b>	<b>0.9962</b>	<b>12.124</b>	<b>0.531</b>	<b>3.541</b>	<b>3.77</b>	<b>0.974, 1.023, 0.994</b>
	0.0	0.9983	12.819	0.578	2.844	3.46	0.977, 1.019, 0.995
	<b>0.3</b>	<b>1.0001</b>	<b>3.229</b>	<b>0.831</b>	<b>4.349</b>	<b>2.41</b>	<b>0.991, 1.008, 0.999</b>
0.8	-0.3	0.9956	15.007	0.476	3.006	4.20	0.969, 1.028, 0.991
	<b>0.0</b>	<b>0.9982</b>	<b>16.162</b>	<b>0.521</b>	<b>2.400</b>	<b>3.84</b>	<b>0.973, 1.023, 0.992</b>
	0.3	1.0001	3.304	0.804	4.224	2.49	0.989, 1.009, 0.998
$\nu=1, \xi=2\%, \mu=0.5\%$							
0.6	-0.3	0.9939	21.256	0.505	2.614	3.97	0.971, 1.025, 0.992
	<b>0.0</b>	<b>0.9970</b>	<b>22.230</b>	<b>0.551</b>	<b>2.113</b>	<b>3.63</b>	<b>0.974, 1.020, 0.992</b>
	0.3	1.0004	6.000	0.798	3.124	2.51	0.989, 1.009, 0.998
0.7	<b>-0.3</b>	<b>0.9933</b>	<b>28.164</b>	<b>0.440</b>	<b>2.116</b>	<b>4.55</b>	<b>0.965, 1.031, 0.987</b>
	0.0	0.9973	29.258	0.485	1.726	4.13	0.968, 1.024, 0.988
	<b>0.3</b>	<b>1.0005</b>	<b>6.254</b>	<b>0.765</b>	<b>2.994</b>	<b>2.61</b>	<b>0.987, 1.010, 0.997</b>
0.8	-0.3	0.9923	35.941	0.387	1.759	5.16	0.958, 1.037, 0.981
	<b>0.0</b>	<b>0.9971</b>	<b>37.599</b>	<b>0.429</b>	<b>1.428</b>	<b>4.67</b>	<b>0.962, 1.029, 0.983</b>
	0.3	1.0004	6.465	0.732	2.874	2.73	0.985, 1.011, 0.997

Table 2 Optimal parameters for non-uniform TLCDC designs in pitching motion with  $\nu = 2$

$\nu = 2, \xi = 1\%, \mu = 0.25\%$							
$p$ (1)	$q$ (2)	$\frac{1}{\beta_{1opt}} = \frac{\omega_d}{\omega_s}$ (3)	$\eta_{opt} (\times 10^{-2}/\hat{M}_0)$	$[\alpha_p]_{norm}$	$[\hat{y}_p]_{norm}$	$\xi_c(\%)$	$k_{1,2,3} = \omega_{1,2,3}/\omega_d$
0.6	-0.3	0.9964	11.843	0.325	1.771	3.08	0.974, 1.023, 0.987
	<b>0.0</b>	<b>0.9983</b>	<b>16.204</b>	<b>0.321</b>	<b>1.323</b>	<b>3.11</b>	<b>0.972, 1.022, 0.986</b>
	0.3	1.0009	7.633	0.426	1.857	2.35	0.981, 1.015, 0.993
0.7	<b>-0.3</b>	<b>0.9961</b>	<b>19.435</b>	<b>0.270</b>	<b>1.260</b>	<b>3.71</b>	<b>0.966, 1.028, 0.982</b>
	0.0	0.9986	25.808	0.267	0.955	3.74	0.964, 1.027, 0.979
	<b>0.3</b>	<b>1.0012</b>	<b>9.585</b>	<b>0.382</b>	<b>1.562</b>	<b>2.62</b>	<b>0.978, 1.017, 0.990</b>
0.8	-0.3	0.9955	31.202	0.226	0.913	4.43	0.958, 1.035, 0.975
	<b>0.0</b>	<b>0.9986</b>	<b>41.907</b>	<b>0.223</b>	<b>0.687</b>	<b>4.49</b>	<b>0.956, 1.033, 0.972</b>
	0.3	1.0014	12.846	0.341	1.279	2.93	0.974, 1.020, 0.987
$\nu = 2, \xi = 1\%, \mu = 0.5\%$							
0.6	-0.3	0.9932	29.921	0.253	0.987	3.96	0.963, 1.030, 0.978
	<b>0.0</b>	<b>0.9969</b>	<b>40.710</b>	<b>0.249</b>	<b>0.737</b>	<b>4.03</b>	<b>0.960, 1.028, 0.975</b>
	0.3	1.0020	18.536	0.339	1.063	2.95	0.973, 1.019, 0.986
0.7	<b>-0.3</b>	<b>0.9927</b>	<b>50.354</b>	<b>0.206</b>	<b>0.690</b>	<b>4.85</b>	<b>0.952, 1.038, 0.970</b>
	0.0	0.9976	67.631	0.204	0.520	4.91	0.949, 1.035, 0.966
	<b>0.3</b>	<b>1.0026</b>	<b>24.217</b>	<b>0.299</b>	<b>0.875</b>	<b>3.34</b>	<b>0.968, 1.022, 0.982</b>
0.8	-0.3	0.9915	82.096	0.171	0.495	5.85	0.940, 1.046, 0.961
	<b>0.0</b>	<b>0.9978</b>	<b>111.504</b>	<b>0.168</b>	<b>0.370</b>	<b>5.96</b>	<b>0.935, 1.041, 0.955</b>
	0.3	1.0030	32.303	0.264	0.712	3.78	0.963, 1.025, 0.977
$\nu = 2, \xi = 2\%, \mu = 0.25\%$							
0.6	-0.3	0.9958	16.797	0.503	2.642	3.98	0.971, 1.025, 0.992
	<b>0.0</b>	<b>0.9977</b>	<b>22.357</b>	<b>0.498</b>	<b>1.995</b>	<b>4.02</b>	<b>0.970, 1.024, 0.989</b>
	0.3	1.0006	11.976	0.612	2.542	3.27	0.979, 1.017, 0.995
0.7	<b>-0.3</b>	<b>0.9952</b>	<b>26.068</b>	<b>0.435</b>	<b>1.970</b>	<b>4.60</b>	<b>0.964, 1.031, 0.986</b>
	0.0	0.9979	34.373	0.432	1.497	4.64	0.962, 1.029, 0.983
	<b>0.3</b>	<b>1.0008</b>	<b>14.426</b>	<b>0.567</b>	<b>2.218</b>	<b>3.53</b>	<b>0.976, 1.019, 0.993</b>
0.8	-0.3	0.9943	39.417	0.377	1.490	5.31	0.956, 1.037, 0.979
	<b>0.0</b>	<b>0.9978</b>	<b>53.379</b>	<b>0.373</b>	<b>1.118</b>	<b>5.37</b>	<b>0.953, 1.035, 0.975</b>
	0.3	1.0010	18.403	0.522	1.884	3.84	0.972, 1.022, 0.991
$\nu = 2, \xi = 2\%, \mu = 0.5\%$							
0.6	-0.3	0.9924	39.217	0.413	1.569	4.85	0.960, 1.032, 0.982
	<b>0.0</b>	<b>0.9963</b>	<b>53.295</b>	<b>0.407</b>	<b>1.174</b>	<b>4.91</b>	<b>0.958, 1.031, 0.979</b>
	0.3	1.0016	26.253	0.518	1.573	3.86	0.971, 1.021, 0.989
0.7	<b>-0.3</b>	<b>0.9915</b>	<b>62.536</b>	<b>0.350</b>	<b>1.145</b>	<b>5.73</b>	<b>0.950, 1.040, 0.973</b>
	0.0	0.9968	84.482	0.346	0.861	5.80	0.947, 1.037, 0.969
	<b>0.3</b>	<b>1.0022</b>	<b>33.193</b>	<b>0.472</b>	<b>1.335</b>	<b>4.24</b>	<b>0.966, 1.024, 0.985</b>
0.8	-0.3	0.9902	98.346	0.298	0.847	6.72	0.937, 1.048, 0.963
	<b>0.0</b>	<b>0.9969</b>	<b>134.269</b>	<b>0.293</b>	<b>0.632</b>	<b>6.83</b>	<b>0.933, 1.044, 0.957</b>
	0.3	1.0026	43.277	0.428	1.115	4.68	0.960, 1.027, 0.980

Table 3 Optimal parameters for non-uniform TLCD designs in pitching motion with  $\nu=3$ 

$\nu=3, \xi=1\%, \mu=0.25\%$							
$p$ (1)	$q$ (2)	$\frac{1}{\beta_{1opt}} = \frac{\omega_d}{\omega_s}$ (3)	$\eta_{opt} (\times 10^{-2}/\hat{M}_0)$	$[\alpha_p]_{norm}$	$[\hat{y}_p]_{norm}$	$\xi_c(\%)$	$k_{1,2,3}=\omega_{1,2,3}/\omega_d$
0.6	-0.3	0.9958	18.447	0.281	1.268	3.56	0.968, 1.027, 0.982
	<b>0.0</b>	<b>0.9980</b>	<b>28.381</b>	<b>0.262</b>	<b>0.904</b>	<b>3.81</b>	<b>0.964, 1.028, 0.979</b>
	0.3	1.0014	17.068	0.319	1.145	3.14	0.971, 1.021, 0.985
0.7	<b>-0.3</b>	<b>0.9954</b>	<b>33.202</b>	<b>0.229</b>	<b>0.857</b>	<b>4.36</b>	<b>0.958, 1.034, 0.857</b>
	0.0	0.9984	49.751	0.215	0.620	4.66	0.953, 1.034, 0.970
	<b>0.3</b>	<b>1.0019</b>	<b>23.900</b>	<b>0.280</b>	<b>0.909</b>	<b>3.57</b>	<b>0.966, 1.025, 0.981</b>
0.8	-0.3	0.9946	58.819	0.188	0.586	5.32	0.947, 1.041, 0.966
	<b>0.0</b>	<b>0.9986</b>	<b>88.678</b>	<b>0.176</b>	<b>0.422</b>	<b>5.70</b>	<b>0.940, 1.041, 0.959</b>
	0.3	1.0023	34.787	0.244	0.704	4.09	0.959, 1.028, 0.975
$\nu=3, \xi=1\%, \mu=0.5\%$							
0.6	-0.3	0.9920	47.672	0.216	0.697	4.64	0.954, 1.035, 0.971
	<b>0.0</b>	<b>0.9964</b>	<b>74.541</b>	<b>0.200</b>	<b>0.492</b>	<b>5.01</b>	<b>0.947, 1.035, 0.965</b>
	0.3	1.0030	43.343	0.245	0.633	4.08	0.959, 1.027, 0.974
0.7	<b>-0.3</b>	<b>0.9914</b>	<b>87.640</b>	<b>0.174</b>	<b>0.465</b>	<b>5.76</b>	<b>0.940, 1.044, 0.960</b>
	0.0	0.9974	133.382	0.162	0.333	6.20	0.931, 1.042, 0.952
	<b>0.3</b>	<b>1.0041</b>	<b>62.254</b>	<b>0.213</b>	<b>0.494</b>	<b>4.70</b>	<b>0.951, 1.031, 0.968</b>
0.8	-0.3	0.9901	159.077	0.142	0.314	7.08	0.923, 1.053, 0.946
	<b>0.0</b>	<b>0.9983</b>	<b>243.320</b>	<b>0.131</b>	<b>0.224</b>	<b>7.65</b>	<b>0.910, 1.048, 0.934</b>
	0.3	1.0051	92.350	0.184	0.378	5.44	0.941, 1.035, 0.959
$\nu=3, \xi=2\%, \mu=0.25\%$							
0.6	-0.3	0.9950	25.052	0.449	1.963	4.46	0.965, 1.029, 0.987
	<b>0.0</b>	<b>0.9973</b>	<b>37.703</b>	<b>0.425</b>	<b>1.422</b>	<b>4.71</b>	<b>0.961, 1.030, 0.983</b>
	0.3	1.0009	23.918	0.495	1.719	4.04	0.969, 1.023, 0.989
0.7	<b>-0.3</b>	<b>0.9943</b>	<b>42.047</b>	<b>0.381</b>	<b>1.395</b>	<b>5.25</b>	<b>0.956, 1.036, 0.978</b>
	0.0	0.9975	62.322	0.361	1.020	5.54	0.951, 1.036, 0.973
	<b>0.3</b>	<b>1.0013</b>	<b>32.313</b>	<b>0.448</b>	<b>1.407</b>	<b>4.47</b>	<b>0.964, 1.027, 0.984</b>
0.8	-0.3	0.9934	72.420	0.323	0.983	6.20	0.944, 1.044, 0.969
	<b>0.0</b>	<b>0.9976</b>	<b>107.716</b>	<b>0.305</b>	<b>0.717</b>	<b>6.57</b>	<b>0.937, 1.043, 0.962</b>
	0.3	1.0017	45.277	0.401	1.125	4.99	0.957, 1.031, 0.978
$\nu=3, \xi=2\%, \mu=0.5\%$							
0.6	-0.3	0.9910	60.345	0.363	1.143	5.52	0.952, 1.038, 0.974
	<b>0.0</b>	<b>0.9955</b>	<b>91.675</b>	<b>0.340</b>	<b>0.821</b>	<b>5.89</b>	<b>0.945, 1.037, 0.967</b>
	0.3	1.0026	57.086	0.402	1.007	4.97	0.956, 1.029, 0.977
0.7	<b>-0.3</b>	<b>0.9902</b>	<b>105.863</b>	<b>0.302</b>	<b>0.792</b>	<b>6.63</b>	<b>0.937, 1.046, 0.963</b>
	0.0	0.9963	158.325	0.284	0.574	7.07	0.929, 1.044, 0.953
	<b>0.3</b>	<b>1.0035</b>	<b>78.566</b>	<b>0.359</b>	<b>0.811</b>	<b>5.59</b>	<b>0.948, 1.033, 0.970</b>
0.8	-0.3	0.9885	184.932	0.252	0.551	7.95	0.920, 1.055, 0.947
	<b>0.0</b>	<b>0.9970</b>	<b>281.161</b>	<b>0.236</b>	<b>0.397</b>	<b>8.51</b>	<b>0.908, 1.051, 0.935</b>
	0.3	1.0044	113.337	0.317	0.637	6.33	0.938, 1.037, 0.961

Table 4 Optimal parameters for non-uniform TLCDC designs in pitching motion with  $\nu = 0.6$

$\nu = 0.6, \xi = 1\%, \mu = 0.5\%$							
$p$ (1)	$q$ (2)	$\frac{1}{\beta_{1opt}} = \frac{\omega_d}{\omega_s}$ (3)	$\eta_{opt} (\times 10^{-2}/\hat{M}_0)$	$[\alpha_p]_{norm}$	$[\hat{y}_p]_{norm}$	$\xi_c(\%)$	$k_{1,2,3} = \omega_{1,2,3}/\omega_d$
0.6	-0.3	0.9951	9.905	0.388	2.627	2.58	0.979, 1.018, 0.992
	<b>-0.15</b>	<b>0.9959</b>	<b>10.305</b>	<b>0.413</b>	<b>2.304</b>	<b>2.42</b>	<b>0.981, 1.017, 0.993</b>
	0.0	0.9975	7.599	0.488	2.391	2.05	0.985, 1.013, 0.996
0.7	-0.3	<b>0.9949</b>	<b>11.865</b>	<b>0.331</b>	<b>2.213</b>	<b>3.02</b>	<b>0.975, 1.023, 0.988</b>
	<b>-0.15</b>	0.9959	12.748	0.351	1.908	2.85	0.976, 1.021, 0.989
	0.0	<b>0.9977</b>	<b>8.931</b>	<b>0.425</b>	<b>2.048</b>	<b>2.35</b>	<b>0.981, 1.015, 0.993</b>
0.8	-0.3	0.9944	13.653	0.288	1.925	3.47	0.970, 1.028, 0.985
	<b>-0.15</b>	<b>0.9956</b>	<b>15.084</b>	<b>0.303</b>	<b>1.632</b>	<b>3.30</b>	<b>0.971, 1.025, 0.986</b>
	0.0	0.9977	10.300	0.373	1.785	2.68	0.977, 1.018, 0.990
$\nu = 0.6, \xi = 1\%, \mu = 1\%$							
0.6	-0.3	0.9905	24.334	0.307	1.498	3.26	0.971, 1.024, 0.985
	<b>-0.15</b>	<b>0.9921</b>	<b>25.103</b>	<b>0.329</b>	<b>1.323</b>	<b>3.04</b>	<b>0.973, 1.021, 0.986</b>
	0.0	0.9952	18.175	0.398	1.401	2.51	0.979, 1.016, 0.990
0.7	-0.3	<b>0.9902</b>	<b>30.059</b>	<b>0.258</b>	<b>1.236</b>	<b>3.88</b>	<b>0.965, 1.031, 0.980</b>
	<b>-0.15</b>	0.9921	32.113	0.275	1.071	3.64	0.966, 1.027, 0.981
	0.0	<b>0.9957</b>	<b>21.937</b>	<b>0.339</b>	<b>1.174</b>	<b>2.95</b>	<b>0.973, 1.020, 0.986</b>
0.8	-0.3	0.9893	34.669	0.221	1.066	4.52	0.958, 1.037, 0.975
	<b>-0.15</b>	<b>0.9916</b>	<b>38.237</b>	<b>0.234</b>	<b>0.906</b>	<b>4.27</b>	<b>0.960, 1.033, 0.976</b>
	0.0	0.9957	25.798	0.293	1.006	3.42	0.968, 1.024, 0.982
$\nu = 0.6, \xi = 2\%, \mu = 0.5\%$							
0.6	-0.3	0.9945	14.910	0.574	3.725	3.49	0.977, 1.020, 0.996
	<b>-0.15</b>	<b>0.9954</b>	<b>15.883</b>	<b>0.600</b>	<b>3.200</b>	<b>3.34</b>	<b>0.978, 1.018, 0.996</b>
	0.0	0.9972	12.572	0.673	3.119	2.97	0.983, 1.014, 0.997
0.7	-0.3	<b>0.9940</b>	<b>16.900</b>	<b>0.510</b>	<b>3.289</b>	<b>3.92</b>	<b>0.973, 1.025, 0.993</b>
	<b>-0.15</b>	0.9953	18.518	0.533	2.788	3.75	0.974, 1.023, 0.993
	0.0	<b>0.9974</b>	<b>13.877</b>	<b>0.612</b>	<b>2.819</b>	<b>3.27</b>	<b>0.979, 1.017, 0.995</b>
0.8	-0.3	0.9934	18.263	0.458	2.986	4.37	0.968, 1.030, 0.989
	<b>-0.15</b>	<b>0.9947</b>	<b>20.515</b>	<b>0.477</b>	<b>2.495</b>	<b>4.20</b>	<b>0.969, 1.027, 0.990</b>
	0.0	0.9972	15.258	0.557	2.561	3.59	0.975, 1.020, 0.994
$\nu = 0.6, \xi = 2\%, \mu = 1\%$							
0.6	-0.3	0.9898	33.820	0.482	2.273	4.15	0.969, 1.026, 0.990
	<b>-0.15</b>	<b>0.9916</b>	<b>35.583</b>	<b>0.508</b>	<b>1.972</b>	<b>3.94</b>	<b>0.970, 1.024, 0.990</b>
	0.0	0.9950	27.494	0.584	1.970	3.42	0.976, 1.017, 0.993
0.7	-0.3	<b>0.9893</b>	<b>39.693</b>	<b>0.420</b>	<b>1.956</b>	<b>4.76</b>	<b>0.962, 1.033, 0.985</b>
	<b>-0.15</b>	0.9913	42.329	0.442	1.680	4.53	0.964, 1.029, 0.985
	0.0	<b>0.9953</b>	<b>31.368</b>	<b>0.520</b>	<b>1.733</b>	<b>3.85</b>	<b>0.971, 1.022, 0.990</b>
0.8	-0.3	0.9882	44.267	0.371	1.739	5.40	0.956, 1.040, 0.980
	<b>-0.15</b>	<b>0.9906</b>	<b>48.897</b>	<b>0.389</b>	<b>1.466</b>	<b>5.15</b>	<b>0.957, 1.035, 0.979</b>
	0.0	0.9951	34.754	0.464	1.550	4.31	0.965, 1.026, 0.986

Table 5 Optimal parameters for non-uniform TLCD designs in pitching motion with  $\nu=0.3$ 

$\nu=0.3, \xi=1\%, \mu=0.1\%$							
$p$ (1)	$q$ (2)	$\frac{1}{\beta_{1opt}} = \frac{\omega_d}{\omega_s}$ (3)	$\eta_{opt} (\times 10^{-2}/\hat{M}_0)$	$[\alpha_p]_{norm}$	$[\hat{y}_p]_{norm}$	$\xi_e(\%)$	$k_{1,2,3}=\omega_{1,2,3}/\omega_d$
0.6	-0.3	0.9912	15.286	0.390	2.606	2.57	0.979, 1.018, 0.992
	<b>-0.15</b>	<b>0.9925</b>	<b>14.273</b>	<b>0.441</b>	<b>2.356</b>	<b>2.27</b>	<b>0.982, 1.015, 0.994</b>
	0.0	0.9951	7.067	0.594	2.753	1.68	0.989, 1.009, 0.998
0.7	-0.3	<b>0.9914</b>	<b>15.710</b>	<b>0.335</b>	<b>2.382</b>	<b>2.99</b>	<b>0.975, 1.023, 0.989</b>
	<b>-0.15</b>	0.9928	14.483	0.379	2.158	2.64	0.978, 1.019, 0.991
	0.0	<b>0.9954</b>	<b>6.975</b>	<b>0.531</b>	<b>2.617</b>	<b>1.88</b>	<b>0.986, 1.011, 0.997</b>
0.8	-0.3	0.9910	14.932	0.289	2.264	3.46	0.971, 1.028, 0.985
	<b>-0.15</b>	<b>0.9926</b>	<b>14.222</b>	<b>0.329</b>	<b>2.025</b>	<b>3.04</b>	<b>0.974, 1.023, 0.988</b>
	0.0	0.9953	6.414	0.475	2.562	2.11	0.984, 1.013, 0.995
$\nu=0.3, \xi=1\%, \mu=2\%$							
0.6	-0.3	0.9831	37.916	0.310	1.491	3.22	0.971, 1.024, 0.985
	<b>-0.15</b>	<b>0.9853</b>	<b>33.500</b>	<b>0.356</b>	<b>1.385</b>	<b>2.81</b>	<b>0.975, 1.019, 0.987</b>
	0.0	0.9904	16.370	0.502	1.676	1.99	0.984, 1.011, 0.995
0.7	-0.3	<b>0.9833</b>	<b>39.021</b>	<b>0.262</b>	<b>1.347</b>	<b>3.82</b>	<b>0.965, 1.030, 0.981</b>
	<b>-0.15</b>	0.9859	35.538	0.301	1.234	3.33	0.969, 1.024, 0.984
	0.0	<b>0.9909</b>	<b>16.247</b>	<b>0.440</b>	<b>1.566</b>	<b>2.28</b>	<b>0.981, 1.014, 0.993</b>
0.8	-0.3	0.9828	38.429	0.224	1.255	4.48	0.960, 1.038, 0.977
	<b>-0.15</b>	<b>0.9857</b>	<b>35.370</b>	<b>0.257</b>	<b>1.141</b>	<b>3.90</b>	<b>0.964, 1.030, 0.979</b>
	0.0	0.9909	15.280	0.386	1.503	2.59	0.978, 1.017, 0.990
$\nu=0.3, \xi=2\%, \mu=1\%$							
0.6	-0.3	0.9907	23.0186	0.576	3.694	3.47	0.977, 1.020, 0.995
	<b>-0.15</b>	<b>0.9921</b>	<b>22.460</b>	<b>0.629</b>	<b>3.203</b>	<b>3.18</b>	<b>0.980, 1.017, 0.996</b>
	0.0	0.9950	13.154	0.764	3.273	2.62	0.987, 1.010, 0.998
0.7	-0.3	<b>0.9906</b>	<b>21.858</b>	<b>0.515</b>	<b>3.563</b>	<b>3.89</b>	<b>0.973, 1.025, 0.993</b>
	<b>-0.15</b>	0.9922	21.579	0.565	3.084	3.54	0.976, 1.021, 0.995
	0.0	<b>0.9952</b>	<b>12.082</b>	<b>0.712</b>	<b>3.289</b>	<b>2.81</b>	<b>0.985, 1.013, 0.997</b>
0.8	-0.3	0.9900	20.370	0.460	3.488	4.35	0.968, 1.030, 0.990
	<b>-0.15</b>	<b>0.9918</b>	<b>19.780</b>	<b>0.508</b>	<b>3.037</b>	<b>3.94</b>	<b>0.972, 1.025, 0.992</b>
	0.0	0.9950	10.788	0.661	3.347	3.03	0.982, 1.015, 0.997
$\nu=0.3, \xi=2\%, \mu=2\%$							
0.6	-0.3	0.9824	52.037	0.487	2.271	4.11	0.969, 1.026, 0.989
	<b>-0.15</b>	<b>0.9849</b>	<b>48.563</b>	<b>0.540</b>	<b>2.023</b>	<b>3.71</b>	<b>0.972, 1.021, 0.991</b>
	0.0	0.9903	27.368	0.687	2.164	2.91	0.982, 1.012, 0.995
0.7	-0.3	<b>0.9824</b>	<b>51.789</b>	<b>0.426</b>	<b>2.125</b>	<b>4.70</b>	<b>0.963, 1.033, 0.985</b>
	<b>-0.15</b>	0.9853	48.791	0.475	1.888	4.22	0.967, 1.026, 0.988
	0.0	<b>0.9907</b>	<b>25.405</b>	<b>0.628</b>	<b>2.136</b>	<b>3.19</b>	<b>0.979, 1.016, 0.994</b>
0.8	-0.3	0.9815	48.404	0.374	2.054	5.35	0.957, 1.040, 0.981
	<b>-0.15</b>	<b>0.9849</b>	<b>46.684</b>	<b>0.419</b>	<b>1.809</b>	<b>4.78</b>	<b>0.962, 1.033, 0.984</b>
	0.0	0.9906	23.006	0.572	2.134	3.50	0.976, 1.019, 0.993

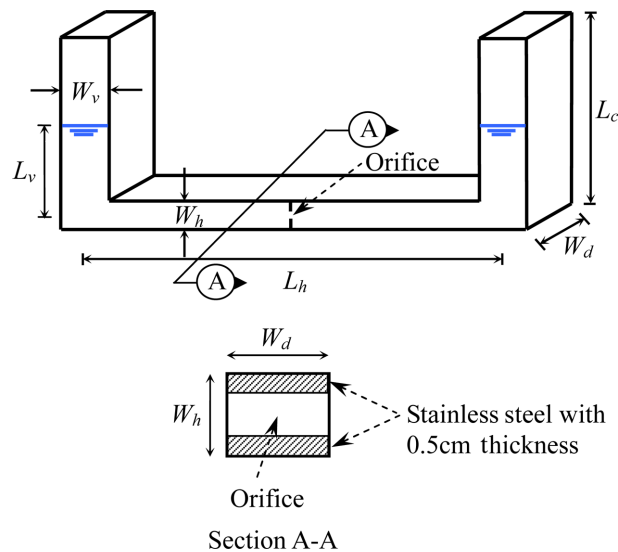


Fig. 4 Schematic dimension diagram of TLCD models

The effect due to the cause (3) can be characterized by the orifice size ratio. The effect of the cause (4) may depend on the dimensions of TLCD containers, such as the out-of-plane width and length of the liquid column. The out-of-plane width effect was observed by Shum and Xu (2002) using an averaging method from the free vibration tests. However, Wu *et al.* (2005) performed forced vibration tests using TLCD models in slightly larger size in a series of combinations of varied out-of-plane widths and horizontal length ratios, and the identified results from comparing the measured data with closed-form solutions intriguingly indicated that (i) the head loss coefficient is insensitive to the ratio of TLCD out-of-plane width versus in-plane width if the ratio is at least equal to 1 or larger; and (ii) the head loss coefficient is insensitive to the horizontal length ratio of the liquid column for the ratio ranging from 0.4 to 0.8, which covers almost all practical designs.

Aside from these, the vibration amplitude is another factor that does not relate to the configuration but might have effect on the head loss coefficient. However, the identification performed by Balendra *et al.* (1995) using the forced vibration tests in different amplitudes had demonstrated that this effect is insignificant.

Based on the observations as above, for the practical design, the TLCD head loss can be summarized as a function of two dominant parameters only, i.e., the cross-sectional ratio and orifice size ratio, regardless of the difference in the dimension of TLCD containers. Therefore, the designer requires the relation link of the head loss coefficient to the cross-sectional ratio and orifice size ratio, which can only be accurately estimated through experimental identification. To further broaden the application spectrum for TLCDs with varied cross-sectional ratios (including uniform and non-uniform TLCDs) in rotational motion, this study inspected a larger extent of different TLCDs with the cross-sectional ratios ranging from 0.3, 0.6, 1, 2 to 3.0 to identify their head loss coefficients by performing a series of tests. A closed-form solution of the liquid response under harmonic rotational base motion was used in the calculation for identifying head loss coefficients. In addition, the insignificance of the liquid vibration amplitude on the head loss coefficient was also indirectly verified by performing forced vibration tests under a white-noise type of base motion. The final objective is to propose design

charts as well as the corresponding empirical formulas for predicting head loss coefficients in relation to the cross-section ratio and orifice size ratio as convenient references for practitioners.

#### 4.1 Closed-form solutions of liquid response under harmonic rotational base motions

Based on Eq. (5) in which the equivalent damping is used, the closed-form amplitude of the liquid response  $y$  under harmonic rotational base motions can be derived as follows. Let the non-dimensional base rotation  $\alpha$  and the non-dimensional liquid response  $\hat{y}$  be substituted by harmonic functions,  $\alpha_0 e^{i2\pi kt}$  and  $\hat{y}_0 e^{i2\pi kt}$ , respectively, in which  $\alpha_0$  and  $\hat{y}_0$  are the non-dimensional amplitude of  $\alpha$  and  $\hat{y}$ . Secondly, knowing the relation  $\varphi_y = |\hat{y}_0|$ , the steady-state amplitude of  $\hat{y}$  (i.e.,  $|\hat{y}_0|$ ) in rotational base motion can be solved and expressed by

$$|\hat{y}_0| = \frac{\sqrt{-2\pi^2(1-k^2)^2 + [4\pi^4(1-k^2)^4 + k^4(8/3\nu n\eta)^2\pi^2(2k^2nr/p-1)^2\alpha_0^2]^{1/2}}}{k^2(8/3\nu n\eta)} \quad (21)$$

Due to the nonlinearity caused by the damping term, the amplitude  $|\hat{y}_0|$  is not linearly dependent on the amplitude of base displacement  $\alpha_0$ . By this formula, the calculation of the steady-state amplitude of liquid response becomes very easy and therefore they will be used for identifying head loss coefficients in comparison with the experimental results. Note that the formula in Eq. (21) is a general expression that can be applied to both uniform and non-uniform TLCDs.

#### 4.2 TLCD test models

As mentioned previously, the TLCD head loss can be dominantly determined by two factors, i.e., the cross-sectional ratio  $\nu$  and orifice blocking ratio, from the view of practical design. The effect of the out-of-plane width and horizontal length ratio  $p$  on the value of head loss coefficient is not significant. Therefore five different designs of TLCD models with five various cross-sectional ratios ( $\nu=0.3, 0.6, 1, 2, 3$ ), each one has five various orifice blocking ratios ( $\psi=0\%, 20\%, 40\%, 60\%$  and  $80\%$ ), were constructed in order to systematically identify their head loss coefficients. Their dimensions and detail configurations are depicted in Table 6 and Fig. 4. The theoretical frequency  $\omega_d = (2g/L_e)^{1/2}$  for each model was also calculated in Table 6 for comparison later. Rectangular cross-section and sharp-edged elbow in design were taken by their simplicity in manufacturing.

#### 4.3 Test setup and procedure

Although the identification for head loss coefficients in forced vibration tests is the main task, the other important property of TLCD, i.e., the natural frequency was also experimentally verified through free vibration tests performed in the structural laboratory of Department of Civil Engineering, National Chiao-Tung University, Taiwan. Shown in Fig. 5 is the TLCDS on the rotational base platform driven by the hydraulic actuator at the right side. Firstly, the TLCDS were sequentially placed on the base platform that was harmonically driven in the same amplitude but various frequencies. The amplitude used in the rotational base motions is 0.03 radians. The effect of the amplitude on the head loss coefficient will be discussed in the section 4.5. The time histories of liquid responses were then recorded by a wave probe resided in the vertical column, while the base displacement is recorded by a LVDT sensor in the actuator. The recorded time should last for a duration long enough to include the

Table 6 Configurations of TLCD Models

Configuration (1)	TLCD ( $\nu=0.3$ ) (2)	TLCD ( $\nu=0.6$ ) (3)	TLCD ( $\nu=1$ ) (4)	TLCD ( $\nu=2$ ) (5)	TLCD ( $\nu=3$ ) (6)
$W_v$ (cm)	4.58	9	15	30	45
$W_h$ (cm)	15	15	15	15	15
$W_d$ (cm)	15	15	15	15	15
$A_v$ (cm <sup>2</sup> )= $W_v \times W_d$	$4.58 \times 15$	$9 \times 15$	$15 \times 15$	$30 \times 15$	$45 \times 15$
$A_h$ (cm <sup>2</sup> )= $W_h \times W_d$	$15 \times 15$	$15 \times 15$	$15 \times 15$	$15 \times 15$	$15 \times 15$
$\nu=A_v/A_h$	0.3	0.6	1	2	3
$L_c$ (cm)	100	100	100	100	100
$L_h$ (cm)	185.4	181	175	145	145
$L_v$ (cm)	48.33	48.33	37.5	48.33	48.33
$L=L_h+2L_v$ (cm)	282.06	277.66	250	241.66	241.66
$L_c=\nu L_h+2L_v$ (cm)	153.21	205.26	250	386.66	531.66
$p=L_h/L$	0.657	0.652	0.7	0.6	0.6
$e$ (cm)	-62.5	-62.5	-62.5	-62.5	-62.5
$q=e/L_h$	-0.345	-0.345	-0.357	-0.431	-0.431
Blocking Ratio $\psi$ (%)	0, 20, 40, 60, 80	0, 20, 40, 60, 80	0, 20, 40, 60, 80	0, 20, 40, 60, 80	0, 20, 40, 60, 80
Theoretical Natural Frequency $\omega_d = (2g/L_c)^{1/2}$ (rad/sec)	$0.57 \times 2\pi$	$0.49 \times 2\pi$	$0.45 \times 2\pi$	$0.36 \times 2\pi$	$0.31 \times 2\pi$



Fig. 5 Picture of a TLCD on the rotational base

free vibration part in the tail. The natural frequency of each TLCD was determined from the measured data in the free vibration part, while the head loss coefficient can be identified using the measured data in the forced vibration part. The same test procedures were repeated until all sets of different orifice blocking ratios were completed.

#### 4.4 Natural frequencies

The natural frequencies of each TLCD model were determined by measuring the peak-to-peak duration in the time history of free vibration for the case of 0% orifice blocking ratio (i.e., the case with

Table 7 Identified natural frequencies of TLCD models

TLCD model (1)	Identified natural frequency (rad/sec) (2)
TLCD ( $\nu=0.3$ )	$0.5871 \times 2\pi$ (2.92%)
TLCD ( $\nu=0.6$ )	$0.4977 \times 2\pi$ (1.55%)
TLCD ( $\nu=1$ )	$0.4505 \times 2\pi$ (0.10%)
TLCD ( $\nu=2$ )	$0.3722 \times 2\pi$ (3.27%)
TLCD ( $\nu=3$ )	$0.3251 \times 2\pi$ (4.64%)

minimal energy dissipation). Shown in Table 7 is the natural frequencies identified for each TLCD model. These identified frequencies are closest to the theoretical frequencies (see Table 6) for uniform TLCDs ( $\nu=1$ ) within 0.2% of estimation error (see the values in the parentheses in Table 7), and a bit shifted for other non-uniform TLCDs. However, the estimation errors are still within 2.9% for TLCDs ( $\nu=0.3$ ) and within 4.6% for TLCDs ( $\nu=3$ ). This validates the theoretical formula,  $\omega_d=(2g/L_e)^{1/2}$ , of the natural frequency for both uniform and non-uniform TLCDs.

#### 4.5 Head loss coefficients

The head loss coefficients were identified by comparing the amplitude of the liquid displacement in the measured time histories of forced vibration tests with those from the closed-form solution described in Eq. (21). For each TLCD model with a particular blocking ratio, the measured amplitude of  $\hat{y}$  versus the non-dimensional frequency  $k$  was firstly plotted. By adjusting the value of  $\eta$  in Eq. (21) until the measured liquid amplitude was best curve-fitted, the final value of head loss coefficient  $\eta$  can be determined. The fitted results are shown in Fig. 6, in which the fitted results are denoted by the solid curves while the points with marks are the measured amplitude data. The head loss coefficients thus determined for the five TLCD models in five various blocking ratios are summarized in Table 8. From Table 8, the following observations were made:

(1) For each TLCD model with a particular cross-sectional ratio  $\nu$ , the head loss coefficients monotonically increase with the orifice blocking ratio. This is reasonable because more blocking introduces more head loss.

(2) At a particular blocking ratio, the head loss coefficients monotonically increase with the cross-sectional ratio  $\nu$  when  $\nu$  is larger than 1. This can be reasonably explained because flow passing through non-uniform cross-section induces more head loss due to additional section contraction or enlargement. However, when  $\nu$  is smaller than 1, the trend is indefinite. More studies through the method of computational fluid dynamics (CFD) on the mechanism of producing such a behavior are underway.

Although the tests in different base amplitudes were not performed to examine their effect on the head loss coefficient, the indirect verification tests were conducted by using white-noise type of base motions to justify the head loss coefficients identified previously. The time histories of the experimental results for the cases in white-noise types of rotational base motions were plotted and denoted by the thick black curves in Fig. 7. The numerically simulated results by substituting the previously identified head loss coefficients (based on the tests in base amplitude 0.03 radians) to Eq. (4), in which the original damping form is used, were denoted by the purple thin curves in Fig. 7 for comparison. Due to page limit, only few cases were presented for exemplification. It can be seen from the figures that both curves match quite remarkably. Since the time history of liquid vibration

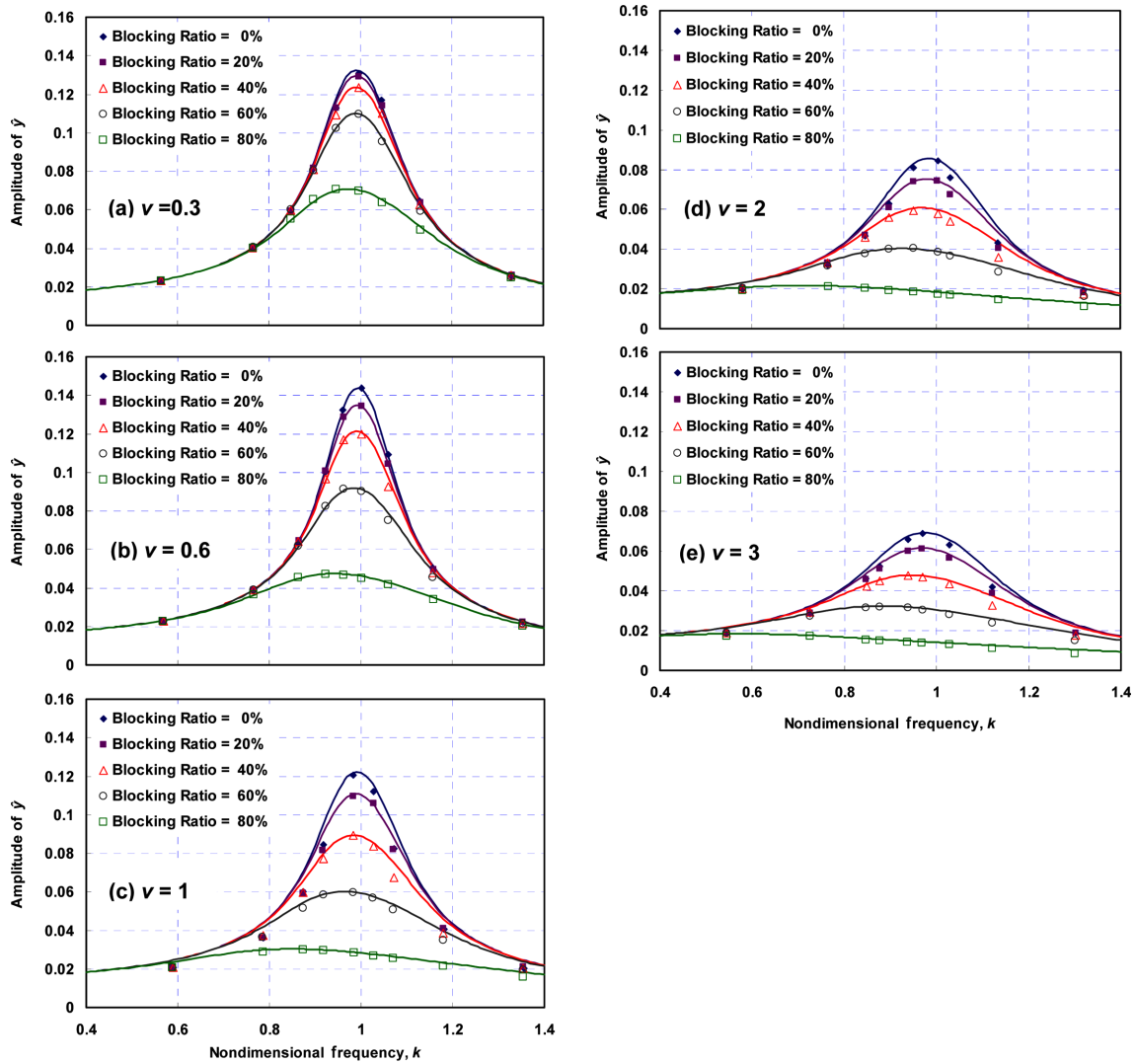


Fig. 6 Comparisons of experimental and fitted results of amplitude  $\hat{y}$  versus dimensionless frequency  $k$  under rotational base motion (base amplitude 0.03 radians): (a)  $\nu=0.3$ , (b)  $\nu=0.6$ , (c)  $\nu=1$ , (d)  $\nu=2$ , and (e)  $\nu=3$

Table 8 Identified head loss coefficients of TLCD models

Blocking ratio $\psi$ (%) (1)	TLCD ( $\nu=0.3$ ) (2)	TLCD ( $\nu=0.6$ ) (3)	TLCD ( $\nu=1$ ) (4)	TLCD ( $\nu=2$ ) (5)	TLCD ( $\nu=3$ ) (6)
0	6.6	3.7	4.1	7.0	9.7
20	6.9	4.2	5.0	9.1	12.4
40	7.6	5.2	7.7	14.1	20.9
60	9.6	9.1	17.3	33.5	49.0
80	23.5	35.7	76.0	149.0	230.0

contains varied amplitudes due to the white-noise excitation, the remarkable correlation shown in Fig. 7 shall indirectly demonstrate that the effect of vibration amplitude on the head loss coefficient

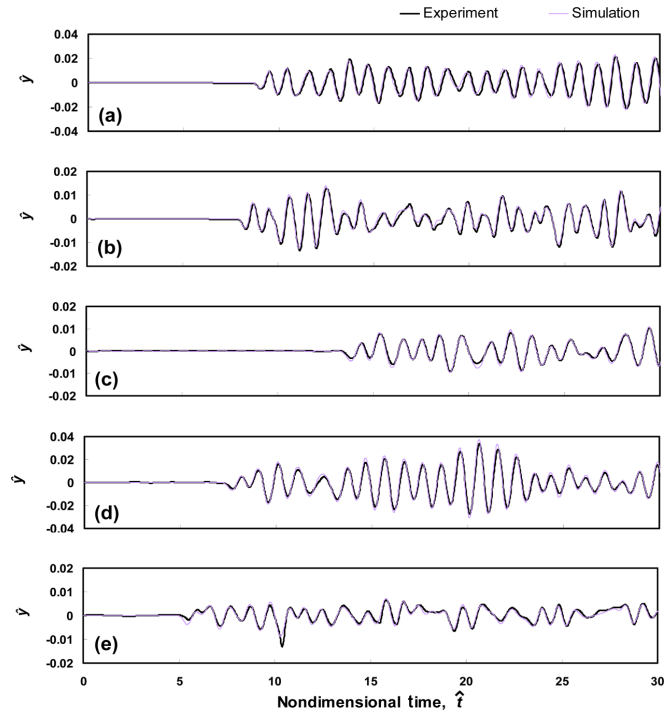


Fig. 7 Time history comparisons of experimental and simulated results in white-noise type of rotational base motion: (a) TLCD ( $\nu=0.3$ ) model with  $\Psi=80\%$ , (b) TLCD ( $\nu=0.6$ ) with  $\Psi=80\%$ , (c) TLCD ( $\nu=1$ ) model with  $\Psi=80\%$ , (d) TLCD ( $\nu=2$ ) model with  $\Psi=0\%$ , and (e) TLCD ( $\nu=3$ ) model with  $\Psi=80\%$

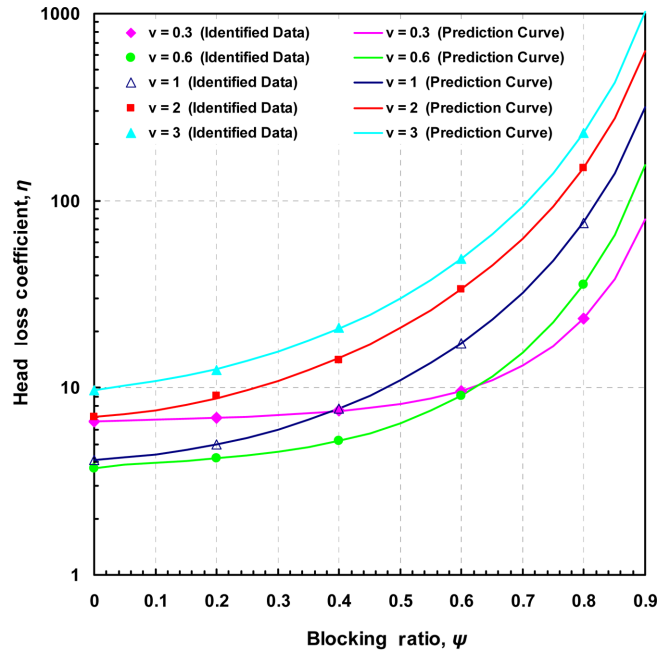


Fig. 8 Comparison of identified data and prediction curves of head loss coefficients in rotational base motion

is insignificant. Therefore, the identified results of the head loss coefficients should be reliable to be used in practice.

Finally, an effort was made to construct the empirical formulas for predicting the head loss coefficients in relation to the cross-sectional ratio and orifice blocking ratio. By minimizing the error between the head loss coefficients identified and prediction curves, the obtained prediction curves are listed as follows.

$$\text{For } \nu=0.3 : \eta = (0.29\psi + 1.77\psi^{4.12})^{0.55}(1-\psi)^{-1.78} + 6.6 \tag{22}$$

$$\text{For } \nu=0.6 : \eta = (0.40\psi + 2.91\psi^{3.46})^{0.48}(1-\psi)^{-2.0} + 3.7 \tag{23}$$

$$\text{For } \nu=1 : \eta = (2.46\psi + 2.17\psi^{1.87})^{1.04}(1-\psi)^{-1.87} + 4.1 \tag{24}$$

$$\text{For } \nu=2 : \eta = (1.59\psi + 3.58\psi^{0.92})^{1.32}(1-\psi)^{-1.91} + 7.0 \tag{25}$$

$$\text{For } \nu=3 : \eta = (1.83\psi + 2.14\psi^{0.44})^{1.79}(1-\psi)^{-1.99} + 9.7 \tag{26}$$

The identified head loss coefficients and the corresponding prediction curves versus the orifice blocking ratios were plotted as a design chart in Fig. 8 for different  $\nu$ . This design chart and the corresponding empirical formulas listed in Eqs. (22)-(26) can provide a valuable reference for practitioners for the practical designs.

### 5. Supplemental information of head loss versus blocking ratio in horizontal motion

According to Wu *et al.* 2005, the steady-state amplitude of  $\hat{y}$  (i.e.,  $|\hat{y}_0|$ ) in horizontal base motion can be solved

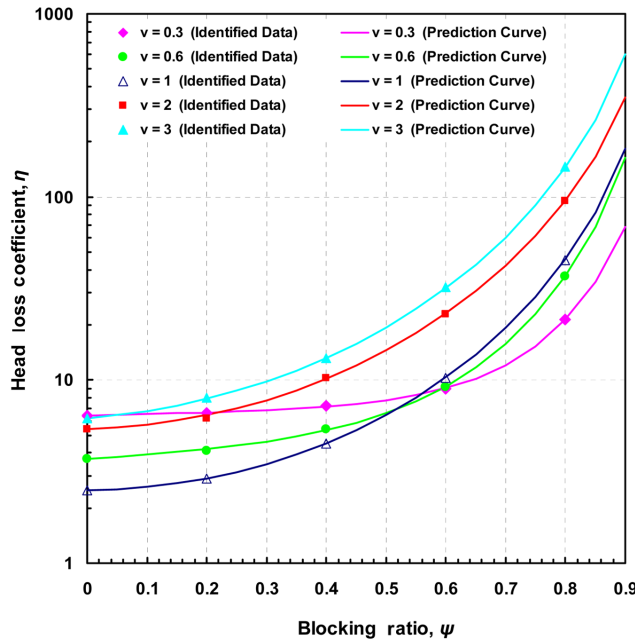


Fig. 9 Comparison of identified data and prediction curves of head loss coefficients in horizontal base motion

$$|\hat{y}_0| = \frac{\sqrt{-2\pi^2(1-k^2)^2 + [4\pi^4(1-k^2)^4 + k^8(8/3\nu n\eta)^2 4\pi^2 n^2 \hat{x}_0^2]^{1/2}}}{k^2(8/3\nu n\eta)} \quad (27)$$

in which  $\hat{x}_0 = x_0/L_h$  is the non-dimensional horizontal base amplitude. Similar to the identification technique used for rotational base motion, the identified head loss coefficients and the corresponding prediction curves versus the orifice blocking ratios were plotted as a design chart in Fig. 9 for different  $\nu$ . This design chart and the corresponding empirical formulas are listed as follows.

$$\text{For } \nu=0.3 : \eta = (0.74\psi + 2.18\psi^{4.86})^{0.92}(1-\psi)^{-1.52} + 6.4 \quad (28)$$

$$\text{For } \nu=0.6 : \eta = (1.32\psi + 1.76\psi^{4.57})^{0.85}(1-\psi)^{-1.90} + 3.7 \quad (29)$$

$$\text{For } \nu=1 : \eta = (1.07\psi + 1.23\psi^{1.15})^{1.46}(1-\psi)^{-1.80} + 2.5 \quad (30)$$

$$\text{For } \nu=2 : \eta = (3.91\psi + 1.38\psi^{2.67})^{1.42}(1-\psi)^{-1.60} + 5.4 \quad (31)$$

$$\text{For } \nu=3 : \eta = (5.44\psi + 1.17\psi^{2.49})^{1.21}(1-\psi)^{-1.85} + 6.2 \quad (32)$$

Eqs. (28)-(32) can provide a valuable reference for practitioners for the practical designs.

## 6. Conclusions

In the first part of the paper, the optimal design parameters, including the frequency tuning ratio, head loss coefficient, the corresponding response and other useful quantities for tuned liquid column dampers (TLCD) in harmonic pitching motion were successfully constructed in design tables as a guideline for practitioners. The configurations in design tables include uniform and non-uniform TLCDs with cross-sectional ratios of 0.3, 0.6, 1, 2 and 3 for the design in different situations. The results from numerical optimization indicates that the optimal structural (pitching) response always occurs when the two resonant peaks along the frequency axis are equal and this applies to both damped and undamped structures.

In the second part of this paper, a systematic experimental investigation to identify the head loss coefficients of TLCDs in various cross-sectional ratios and orifice blocking ratios in rotational base motions were performed. In identification, the closed-form solution of the TLCD liquid response under harmonic base motion were employed. The configurations of TLCD models tested cover the cross-sectional ratios ranging from 0.3, 0.6, 1.0, 2.0 to 3.0 and orifice blocking ratios ranging from 0%, 20%, 40%, 60% to 80%. The identified results of head loss coefficients were plotted as a design chart and it shows that: (1) for each TLCD model with a particular cross-sectional ratio, the head loss coefficients monotonically increase with the orifice blocking ratio; (2) At a particular blocking ratio, the head loss coefficients monotonically increase with the cross-sectional ratio  $\nu$  when  $\nu$  is larger than 1, however, the trend is indefinite when  $\nu$  is smaller than 1. The corresponding empirical formulas (including pitching base motion case and horizontal base motion case) for predicting head loss coefficients of TLCDs in relation to the cross-sectional ratio and orifice blocking ratio were also proposed as quick references for practical designs.

## Acknowledgments

The authors would like to express their gratitude to the financial support of National Science Council of Taiwan under the grant number NSC93-2745-E-032-007.

## References

- Balendra, T., Wang, C.M. and Cheong, H.F. (1995), "Effectiveness of tuned liquid column dampers for vibration control of towers", *Eng. Struct.*, **17**(9), 668-675.
- Balendra, T., Wang, C.M. and Rakesh, G. (1999a), "Effectiveness of TLCD on various structural systems", *Eng. Struct.*, **21**(4), 291-305.
- Balendra, T., Wang, C.M. and Rakesh, G. (1999b), "Vibration control of various types of buildings using TLCD", *J. Wind Eng. Ind. Aerod.*, **83**(1-3), 197-208.
- Chakraborty, S. and Debbarma, R. (2011), "Stochastic earthquake response control of structures by liquid column vibration absorber with uncertain bounded system parameters", *Struct. Saf.*, **33**(2), 136-144
- Chang, C.C. and Hsu, C.T. (1998), "Control performance of liquid column vibration absorbers", *Eng. Struct.*, **20**(7), 580-586.
- Chang, C.C. (1999), "Mass dampers and their optimal designs for building vibration control", *Eng. Struct.*, **21**(5), 454-463.
- Chang, C. H. (2011), "Computational fluid dynamics simulation for tuned liquid column dampers in horizontal motion", *Wind Struct.*, **14**(5), 435-447.
- Debbarma, R., Chakraborty, S. and Kumar, G.S. (2011), "Optimum design of tuned liquid column dampers under stochastic earthquake load considering uncertain bounded system parameters", *Int. J. Mech. Sci.*, **52**(10), 1385-1393.
- Den Hartog, J.P. (1956), *Mechanical Vibrations*, 4<sup>th</sup> Ed., McGraw-Hill, NY.
- Gao, H., Kwok, K.C.S. and Samali, B. (1997), "Optimization of tuned liquid column damper", *Eng. Struct.*, **19**(6), 476-86.
- Heo, J. S., Lee, S.K., Park, E., Lee, S.H., Min, K.W., Kim, H., Jo, J. and Cho, B.H. (2009) "Performance test of a tuned mass damper for reducing bidirectional response of building structures", *Struct. Des. Tall Spec.*, **18**(7), 789-805.
- Hitchcock, P.A., Kwok, K.C.S. and Watkins, R.D. (1997), "Characteristics of liquid column vibration absorbers (LCVA) - I, II", *Eng. Struct.*, **19**, 126-44.
- Li, S. K., Min, K.W. and Lee, H. R. (2011), "Parameter identification of new bidirectional tuned liquid column and sloshing dampers", *J. Sound Vib.*, **330**(7), 1312-1327.
- Sakai, F., Takaeda, S. and Tamaki, T. (1989), "Tuned liquid column damper-new type device for suppression of building vibration", *Proceedings of the International Conference on High-rise Building*, Nanjing, China.
- Shum, K.M. and Xu, Y.L. (2002), "Multiple-tuned liquid column dampers for torsional vibration control of structures: experimental investigation", *Earthq. Eng. Struct. D.*, **31**, 977-991.
- Skelton, R.E. (1988), *Dynamic systems control: Linear systems analysis and synthesis*, Wiley, NY.
- Taflanidis, A.A., Angelides, D.C. and Manos, G.C. (2005), "Optimal design and performance of liquid column mass dampers for rotational vibration control of structures under white noise excitation", *Eng. Struct.*, **27**(4), 524-534.
- Won, A., Pires, J.A. and Haroun, M.A. (1997), "Performance assessment of tuned liquid column dampers under random seismic loading", *Int. J. Nonlinear Mech.*, **32**(4), 745-758.
- Wu, J.C., Shih, M.H., Lin, Y.Y. and Shen, Y.C. (2005), "Design guidelines for tuned liquid column damper for structures responding to wind", *Eng. Struct.*, **27**(13), 1893-1905.
- Wu, J.C., Wang, Y.P., Lee, C.L., Liao, P.H. and Chen, Y.H. (2008), "Wind-induced interaction of a non-uniform tuned liquid column damper and a structure in pitching motion", *Eng. Struct.*, **30**(12), 3555-3565.
- Wu, J.C., Chang, C.H. and Lin, Y.Y. (2009), "Optimal designs for non-uniform tuned liquid column dampers in horizontal motion", *J. Sound Vib.*, **326**(1-2), 104-122.

- Xu, Y.L., Samali, B. and Kwok, K.C.S. (1992), "Control of along-wind response of structures by mass and liquid dampers", *J. Eng. Mech.- ASCE*, **118**(1), 20-39.
- Xu, Y.L. and Shum, K.M. (2003), "Multiple-tuned liquid column dampers for torsional vibration control of structures: theoretical investigation", *Earthq. Eng. Struct. D.*, **32**(2), 309-328.
- Xue, S.D., Ko, J.M. and Xu, Y.L. (2000a), "Tuned liquid column damper for suppressing pitching motion of structures", *Eng. Struct.*, **23**(11), 1538-1551.
- Xue, S.D., Ko, J.M. and Xu, Y.L. (2000b), "Optimum parameters of tuned liquid column damper for suppressing pitching vibration of an undamped structure", *J. Sound Vib.*, **235**(4), 639-653.
- Yalla, S. and Kareem, A. (2000), "Optimum absorber parameters for tuned liquid column dampers", *J. Struct. Eng - ASCE*, **126**(8), 906-915.

CC